TOXICOLOGICAL SCIENCES **132(1)**, 196–210 2013
doi:10.1093/toxsci/kfs339
Advance Access publication January 3, 2013

Toxicity of the Flame-Retardant BDE-49 on Brain Mitochondria and Neuronal Progenitor Striatal Cells Enhanced by a PTEN-Deficient Background

Eleonora Napoli,* Connie Hung,* Sarah Wong,* and Cecilia Giulivi*,†,[1]

*Department of Molecular Biosciences, School of Veterinary Medicine and †Medical Investigations of Neurodevelopmental Disorders (M.I.N.D.) Institute, School of Medicine, University of California, Davis, California 95616

[1]To whom correspondence should be addressed at Department of Molecular Biosciences, University of California, 1 Shields Ave., 1120 Haring Hall, Davis, CA 95616. Fax: (530) 752-4608. E-mail: cgiulivi@ucdavis.edu.

Received September 27, 2012; accepted December 14, 2012

Polybrominated diphenyl ethers (PBDEs) represent an important group of flame retardants extensively used, tonnage of which in the environment has been steadily increasing over the past 25 years. PBDEs or metabolites can induce neurotoxicity and mitochondrial dysfunction (MD) through a variety of mechanisms. Recently, PBDEs with < 5 Br substitutions (i.e., 2,2′,4,4′-tetrabromodiphenyl ether [BDE-47] and 2,2′,4,5′-tetrabromodiphenyl ether [BDE-49]) have gained interest because of their high bioaccumulation. In particular, congeners such as BDE-49 arise as one of the most biologically active, with concentrations typically lower than those observed for BDE-47 in biological tissues; however, its potential to cause MD at biologically relevant concentrations is unknown. To this end, the effect of BDE-49 was studied in brain mitochondria and neuronal progenitor striatal cells (NPC). BDE-49 uncoupled mitochondria at concentrations < 0.1 nM, whereas at > 1 nM, it inhibited the electron transport at Complex V (mixed type inhibition; IC_{50} = 6 nM) and Complex IV (noncompetitive inhibition; IC_{50} = 40 nM). These concentrations are easily achieved in plasma concentrations considering that BDE-49 (this study, 400-fold) and other PBDEs accumulate 1–3 orders of magnitude in the cells, particularly in mitochondria and microsomes. Similar effects were observed in NPC and exacerbated with PTEN (negative modulator of the PI3K/Akt pathway) deficiency, background associated with autism-like behavior, schizophrenia, and epilepsy. PBDE-mediated MD *per se* or enhanced by a background that confers susceptibility to this exposure may have profound implications in the energy balance of brain.

Key Words: **mitochondria; polybrominated diphenyl ethers; Complex IV; bioenergetics; PTEN; autism; epilepsy.**

Polybrominated diphenyl ethers (PBDEs) are a group of high-volume chemicals extensively used in plastics, textiles, furniture, and electronic devices (McDonald, 2002). Studies in the U.S. populations have demonstrated the presence of PBDEs in human breast milk, adipose tissue, and blood (Betts, 2002; Schecter *et al*., 2003). In particular, PBDE levels in northern California women are among the highest levels reported to date (3 to 25 times higher than those in other regions of the world; Petreas *et al*., 2011; She *et al*., 2002), as expected for the San Francisco Bay area, one of the most contaminated regions worldwide (Davis *et al*., 2007; Flegal *et al*., 2007; Luengen *et al*., 2004; Oros *et al*., 2007). PBDEs share structural similarity to the persistent noncoplanar polychlorinated biphenyls, which have been shown to impact individual- (Park *et al*., 2010) and population-level health outcomes (Schwarzenbach *et al*., 2006). PBDEs have high heat stability, high lipid solubility, and low vapor pressure, which contribute to their environmental persistence and bioaccumulation (Darnerud, 2003). In particular, PBDEs with less than five bromine substitutions (i.e., 2,2′,4,4′-tetrabromodiphenyl ether [BDE-47] and 2,2′,4,5′-tetrabromodiphenyl ether [BDE-49]) have recently raised the greatest concern because of their extremely high bioaccumulation (Darnerud *et al*., 2001) and, in the case of BDE-49, for its endogenous generation via debromination of higher substituted PBDEs (Stapleton *et al*., 2006).

Although the mechanisms responsible for PBDE-induced toxicity are not well understood (Costa *et al*., 2008), recent research has focused on the ability of PBDEs to (1) disrupt thyroid hormone status, leading to abnormalities in fetal growth and development in laboratory animals (Birnbaum and Staskal, 2004; Branchi *et al*., 2003; Zhou *et al*., 2002), (2) alter intracellular Ca^{2+} homeostasis especially in excitable cells (Coburn *et al*., 2008; Dingemans *et al*., 2008; Dingemans *et al*., 2010b; Kodavanti and Ward, 2005; Reistad *et al*., 2006; Seo *et al*., 2008), and (3) modulate ryanodine receptors type 1 (RyR1) and type 2 (RyR2) (Kim *et al*., 2011; Pessah *et al*., 2010). Furthermore PBDEs, along with other environmental compounds, have been very recently linked to neurodevelopmental disorders (Herbstman *et al*., 2010), including autism (Hertz-Picciotto *et al*., 2011). In this regard,

the observed seven- to eightfold increase in the incidence of autism in California from the early 1990s through the present and the 23% increase recorded since the last report in 2009 from Center for Disease Control and Prevention (1 in 54 boys and 1 in 252 girls (Baio, 2012)) cannot be attributed solely to changes in diagnostic criteria, the inclusion of milder cases, and an earlier age at diagnosis, suggesting that yet unidentified environmental exposures could contribute to the escalating diagnostic risks (Hertz-Picciotto and Delwiche, 2009). PBDEs seem to be plausible candidates to fit this putative exposure model based on (a) their increased environmental abundance and human exposures (Zota *et al*., 2008) and (b) their activity toward biological targets that mediate important aspects of neuronal development and synaptic plasticity (Dingemans *et al*., 2011; Kim *et al*., 2011).

A growing body of evidence suggests that PBDEs (or their hydroxylated metabolites) can induce mitochondrial dysfunction (MD) by a variety of mechanisms including altering calcium homeostasis (Dingemans *et al*., 2010a; Kodavanti and Ward, 2005), increasing mitochondria depolarization (Hu *et al*., 2009; Shao *et al*., 2008), changing mitochondrial morphology (Talsness *et al*., 2005), triggering apoptosis (Seo *et al*., 2008; Shao et al., 2008), and increasing oxidative stress (Huang *et al*., 2010; Shao *et al*., 2008) in a variety of biological systems.

The goal of this study was to evaluate the mitochondrial toxicity of BDE-49 at low but biologically relevant concentrations such as those reported for BDE-47 in plasma of children living in Mexico and California (0.07–1.8 nM; Eskenazi *et al*., 2011; Hertz-Picciotto *et al*., 2011). BDE-49 is one of the most biologically active PBDE congeners implicated in neurotoxicity and impaired neurodevelopment (Dingemans *et al*., 2011; Kim *et al*., 2011), but, in comparison to the more widely studied tetrabrominated congener BDE-47, limited information is available on its toxicity. No reports had been published on brain accumulation of BDE-49; however, BDE-47 and hydroxylated derivatives had been found in brain in a variety of species originated from transplacental transfer and/or diet, especially during early perinatal periods when the blood-brain barrier has not been completely developed (Naert *et al*., 2007; Ta *et al*., 2011; Wang *et al*., 2011; Zhang *et al*., 2008).

BDE-49 is one of the least abundant congeners in the environment, with levels typically lower than those observed for BDE-47 in fish, wildlife, and human tissues (Mariottini *et al*., 2008; Miller *et al*., 2009; Roosens *et al*., 2008). However, its bioaccumulation may be compounded by the hepatic debromination of higher polybrominated congeners such as BDE-99 (Browne *et al*., 2009; McClain *et al*., 2012; Roberts *et al*., 2011) and the known accumulation of PBDEs in cells (which may vary from 25- to 3400-fold), particularly, in microsomes and mitochondria (Huang *et al*., 2010).

In this study, acute effects of BDE-49 on mitochondrial functions and morphology were evaluated in (1) isolated brain mitochondria from mice aged 21 days, developmental stage in the rodent that reflects the second postnatal year in the human when still brain is developing (Dobbing and Sands, 1979), and (2) neuronal progenitor striatal cells (NPC) from mouse striatum. The relevance of studying NPC is that in the adult brain, the hippocampus and subventricular (SVZ)/olfactory bulb (OB) system exhibit continued plasticity, generating new neurons throughout the lifetime of animals, including the human (Eriksson *et al*., 1998). Newly generated neurons in hippocampus are capable of integrating into neural networks as fully functional neurons (van Praag *et al*., 2002), and they play an important role in hippocampal-dependent spatial learning and memory (Bruel-Jungerman *et al*., 2007; Shors *et al*., 2001). In the SVZ/OB system, NPC differentiate into either granule cells or periglomerular interneurons, where the majority of granular neurons are postnatally produced. The continued production of new neurons throughout life provides a possibility for compensation or repair of certain injuries such as those from BDE-49 exposure. The choice of striatum was made based on recent studies that have shown a strong association between aberrant striatal function and the physiopathology of autism (Di Martino *et al*., 2011; Langen *et al*., 2009; Peça *et al*., 2011).

In addition, we wanted to test how a genetic background relevant to behavior may shape or modulate the toxicity of BDE-49 exposure. This was accomplished by using NPC in which the activity of the lipid phosphatase PTEN, a negative modulator of phosphatidylinositol 3-kinase (PI3K) and Akt pathways, was pharmacologically inhibited. PTEN deficiencies had been linked to autism spectrum disorders (Butler *et al*., 2005; Buxbaum *et al*., 2007; Fraser *et al*., 2008; Goffin *et al*., 2001; Herman *et al*., 2007; Varga *et al*., 2009), aberrant social and repetitive behavior (Butler *et al*., 2005; Buxbaum *et al*., 2007; Goffin *et al*., 2001; Herman *et al*., 2007; Kwon *et al*., 2006; Napoli *et al*., 2012; Varga *et al*., 2009), and, more recently, epilepsy (Pun *et al*., 2012). Although PI3K/Akt activation is required for fundamental processes, a sustained activation of these pathways can result in MD (Napoli *et al*., 2012) with accumulation of mtDNA deletions (Napoli *et al*., 2012) and defective clearance of damaged mitochondria by autophagy or mitophagy (Lee *et al*., 2012; Okamoto and Kondo-Okamoto, 2012) as it has been reported in several disorders with dysregulation of Akt (Gottlieb and Carreira, 2010) and/or PTEN (Garcia-Cao *et al*., 2012; Pun *et al*., 2012).

MATERIALS AND METHODS

Chemicals and biochemical. EDTA, EGTA, cytochrome *c* from bovine heart (no. C2037), HEPES, mannitol, sodium succinate, and sucrose were all purchased from Sigma (St Louis, MO). Tris-HCl, glycine, sodium chloride, and potassium chloride were purchased from Fisher (Pittsburgh, PA). Bovine serum albumin (fatty-acid free) was obtained from MP Biomedicals. BDE-49 (100% pure; AccuStandard, New Haven, CT) was a kind gift from Dr Isaac Pessah (Department of Molecular Biosciences; University of California, Davis). All reagents were of analytical grade.

Isolation of mouse brain mitochondria and evaluation of the mitochondrial fraction purity. Mitochondria from mouse brain (cortex and cerebellum from 21-day-old male mice) were isolated by differential centrifugation and purified through Percoll gradient (Sims and Anderson, 2008) as described in the Supplementary methods and Supplementary figure 1.

Oxygen consumption measurements in isolated, coupled mitochondria from mouse brain. The oxygen uptake of isolated, intact mitochondria was measured with a Clark-type O_2 electrode from Hansatech (King's Lynn, UK) at 22ºC using previously described methods (Elfering *et al*., 2004). All measurements were completed in at least duplicates in 0.22 M sucrose, 50 mM KCl, 5 mM $MgCl_2$, 1 mM EGTA, 10 mM KH_2PO_4, and 10 mM HEPES, pH 7.4 (reaction buffer). Briefly, an aliquot of mitochondria (0.6–1 mg protein/ml) was added to the oxygen chamber that contained 0.5 ml of reaction buffer. Oxygen consumption rates were evaluated in the presence of buffered 1 mM malate and 10 mM glutamate (State 4 oxygen uptake rate) followed by the addition of 1 mM ADP (State 3 oxygen uptake rate). Then, 5 µM rotenone was added, followed by the addition of 10 mM succinate. This oxygen consumption was inhibited by adding 3.6 µM antimycin A. Cytochrome *c* oxidase (CCO) activity (polarographic assay) was evaluated as the (1 mM KCN) KCN-sensitive oxygen uptake in the presence of 10 mM ascorbate and 0.2 mM N,N,N′,N′–tetramethyl-*p*-phenylenediamine. The respiratory control ratio (RCR), considered as the best indicator of membrane integrity of the mitochondrial fraction (Estabrook, 1967), was calculated as the ratio of rates of oxygen uptake in State 3 and State 4.

Cell culture conditions. Conditionally immortalized NPC from mouse striatum ($STHdh^{Q7/Q7}$), obtained from the Coriell Cell Repositories, was used in this study (Trettel *et al*., 2000). Growing conditions were reported in details under Supplementary methods.

Cell harvesting and preparation for oxygen uptake experiments. Medium was aspirated from the T75 flask, and cells were washed once with PBS, pH 7.4. Cells were trypsinized as described above. Approximately 7 ml of growth medium was added; cells were collected and spun down at 500 × g for 5 min. The cell pellet was resuspended in sodium buffer saline (PBS). Membrane integrity was determined with the trypan blue (0.2%) exclusion method and counted with a TC 10 cell counter. Membrane integrity (%) was calculated as the number of trypan blue negative (unstained) cells over the total number of cells present in the field of view according to Tchir and Acker (2010).

Treatment of NPC with BDE-49 and SF1670. NPC were grown in complete growth media for 24 h and then treated with either BDE-49 (0.01–40 nM) or vehicle (0.0004% dimethyl sulfoxide [DMSO]) for 2 h at 33°C. At the end of the incubation, cells were washed with PBS and detached by trypsinization, and membrane integrity was determined as explained above. For the inhibition of PTEN, cells were grown for 24 h and then treated with either 3 nM SF1670 or equivalent volume of vehicle (0.00003% DMSO) for another 24 h at 33°C. At the end of the incubation, addition of BDE-49 or vehicle was performed for 2 h. Cells were finally washed with PBS and detached by trypsinization, and membrane integrity was determined as explained above. Average of cells with intact membrane was 95%—as judged by the trypan blue exclusion method—regardless of the treatment performed. The occurrence of condensed nuclear chromatin (hallmark of apoptosis) was evaluated by analyzing the cells stained with 1 µg/ml 4′,6 diamidino-2-phenylindole (DAPI) as described below (under *Evaluation of mitochondrial distribution and morphology by confocal microscopy*). Images of stained nuclei and DAPI immunofluorescence quantification are shown, respectively, in Supplementary figures 2A and B.

Oxygen consumption by NPC. The oxygen uptake of cells (control, BDE-49 treated, or SF1670 treated) was measured with a Clark-type O_2 electrode from Hansatech at 22°C. Cells (5×10^6) were resuspended in 1 ml of growth media without phenol red. Oxygen rates were recorded for 2 min, followed by the sequential additions of 0.2 µM oligomycin and either 2 µM carbonylcyanide-*p*-trifluoromethoxyphenylhydrazone (FCCP), a potent uncoupler of oxidative phosphorylation (OXPHOS), or various concentrations of BDE-49 (0.2, 2, 20, 40 nM). RCRu is defined as the rate of oxygen uptake in State 3u (with substrate and FCCP) divided by that in oligomycin-inhibited State 4.

Activities of mitochondrial complexes. Protein extracts (for enzymatic analyses) were obtained by resuspending cell pellets (at an equivalent concentration of 5×10^6 cells/ml) or brain mitochondria (2–5 µg) in a hypotonic buffer (20 mM HEPES, pH 7.4) supplemented with phosphatase inhibitors (Sigma no. P0044) and proteolytic inhibitors (Sigma no. P2714), incubating on ice for 10–15 min, and homogenizing the suspension with 30 strokes with a hand homogenizer, followed by two cycles of freezing and thawing. Protein for the enzymatic assays was determined using the BCA assay kit from Pierce (Catalog no. 23227). NADH-decylubiquinone oxidoreductase, succinate cytochrome *c* reductase, ATPase, and citrate synthase activities were evaluated as described before (Giulivi *et al*., 2010; Ross-Inta *et al*., 2010). Details on the measurements of individual Complex activities are reported in the Supplementary methods.

Evaluation of mitochondrial distribution and morphology by confocal microscopy. Cells (1×10^5) were seeded on sterile coverslips, grown overnight at 33°C and then incubated for 24 h with 3 nM SF1670 or vehicle (0.00003% DMSO) at 33°C. Cells were treated with 40 nM BDE-49 or vehicle (0.0004% DMSO) for 2 h at 33°C, followed by incubation with 0.5 µM MitoTracker Red CMXRos (MolecularProbes Inc., Eugene, OR) diluted in growth media for 30 min at 33°C. After staining, cells were washed with media and fixed in 3.7% formaldehyde for 10 min. Fixed cells were washed again in PBS, blocked/permeabilized for 30 min in blocking buffer at 20°C–22°C, counterstained with 1 µg/ml DAPI, and mounted on glass slides with antifading mounting media (Dako). Fluorescent images were obtained using an Olympus FV1000 laser scanning confocal microscope (excitation and emission wavelengths 594 and 660 nm, respectively) with either a 40× or a 60× magnification.

Western blotting. Cells were collected by trypsinization, pelleted by centrifugation at 300 × g for 5 min, extracted in RIPA buffer, and then denatured in NuPAGE sample buffer (Invitrogen) plus 50 mM dithiothreitol (DTT) at 70°C for 10 min. Thirty micrograms of protein were loaded onto 4–12% Bis-Tris gels (Invitrogen) and electrophoresed at 200 V for approximately 45 min. Proteins were then transferred via iBlot system (Invitrogen) to a 0.2-µm nitrocellulose membrane for 7 min (program 3). Antinitrotyrosine antibody (clone 1A6) was from Millipore (Billerica, MA), and the antibody anti-β subunit of mitochondrial ATPase was from BD Biosciences (San Jose, CA). Other experimental details are described in the Supplementary methods.

Quantification of mtDNA copy number per cell and mtDNA deletions by quantitative real-time PCR. For evaluation of mtDNA copy number, quantitative real-time PCR (qPCR) with dual-labeled probes was performed as previously described (Napoli *et al*., 2012). The targeted genes were the single-copy nuclear PK and mitochondrial ND1, ND4, and CYTB. All other details were included in the Supplementary methods.

Statistical and power analyses. The number of experiments per group required to reach statistical significance (with alpha and beta fixed at 0.05 and 0.95) was computed using G*power analysis from an *a priori* analysis. Experiments were run in triplicates, and data were expressed as mean ± SE. The data were evaluated by the ANOVA followed by Bonferroni's posttest for multiple comparisons or by a two-tailed Student *t*-test using StatSimple v2.0.5 (Nidus Technologies, Toronto, Canada) and considering $p \le 0.05$ as statistically significant unless indicated.

RESULTS

BDE-49 Acts as a Mitochondrial Uncoupler and Inhibitor of Complexes IV and V

Purified, coupled brain mitochondria consumed oxygen in the presence of NAD-linked (malate-glutamate) or FAD-linked (succinate) substrates with ADP (phosphorylating mitochondria under State 3) or without ADP (nonphosphorylating mitochondria under State 4). The rates of oxygen uptake of

phosphorylating mitochondria in the presence of malate-glutamate and succinate were 12 ± 2 and 13.6 ± 0.1 nmol oxygen × (min × mg protein)$^{-1}$, respectively. The rate of electron transport was coupled to the synthesis of ATP when using both substrates as it was indicated by the high RCR obtained with each set of substrates (RCR = 6.3 ± 0.2 and 7.2 ± 0.2, respectively).

In the presence of malate-glutamate or succinate, the rates of oxygen uptake in State 4 by brain mitochondria treated with 20 nM BDE-49 were significantly higher than that of vehicle treated (1.4- and 1.6-fold, respectively), whereas the rates of oxygen uptake under State 3 were not affected (Fig. 1A). With the addition of 20 nM BDE-49, the RCR decreased to 2.9 ± 0.1 and 4.9 ± 0.5 with malate-glutamate and succinate, respectively, suggesting that the majority of mitochondria were uncoupled (60–70%; Fig. 1A). Higher concentrations of BDE-49 (40 nM) did not change significantly the rate of oxygen uptake in State 4 but decreased significantly that of State 3 with both substrates (in average by 75%; Fig. 1A). Thus, the decreases in RCR obtained with 40 nM BDE-49 were mainly attributed to the decreases in State 3 oxygen uptake (Fig. 1A). Oxygen uptake by brain mitochondria treated with either 20 or 40 nM BDE-49 remained sensitive to cyanide (inhibitor of Complex IV) or antimycin A (inhibitor of Complex III), and that treated with NAD-linked oxidations to rotenone (not shown).

If BDE-49 were acting as an uncoupler at relatively low concentrations (< 20 nM), it would be expected to release the oligomycin-inhibited State 3 respiration in isolated brain mitochondria. Oxygen uptake by isolated brain mitochondria supported by malate-glutamate was significantly inhibited by addition of 0.2 µM oligomycin (35% of vehicle treated; $p = 0.009$). Addition of 2 µM FCCP increased the rate of oxygen uptake by 8.3-fold ($p = 0.0004$; Fig. 1B). Similarly to FCCP, the rate of oxygen uptake inhibited by oligomycin was partly abrogated by the addition of 0.2 nM BDE-49 (4.1-fold of oligomycin treated; $p = 0.01$) and less evident with 2 nM BDE-49 (twofold; $p = 0.05$). Higher concentrations of BDE-49 (20 and 40 nM) significantly inhibited oxygen uptake (by 45%, $p = 0.002$, and 66%, $p = 0.003$, respectively; Fig. 1B).

Given the similar oxygen uptake inhibition obtained with NAD- and FAD-linked substrates in the presence of 40 nM BDE-49, the effect of this compound could be ascribed to the inhibition of any of the complexes present in the electron transport segment shared by both substrates (i.e., Complexes III and IV) and/or the inhibition of ATPase. To this end, the activities of individual complexes were tested at various concentrations of BDE-49. A significant inhibition was obtained with Complex V (Figs. 1C and D) and Complex IV (Fig. 1E, inset). BDE-49 affected significantly Complex V or the oligomycin-sensitive ATPase activity. Lineweaver-Burk plots of initial rates for hydrolysis of 10 nM–3 mM ATP were biphasic, extrapolating to two apparent K_m values, one of high affinity (of about 5 µM) and the other of low affinity (70 µM). Both K_m were similar to those reported by others using coupled submitochondrial particles (2–4 µM and 120–160 µM; Matsuno-Yagi and Hatefi, 1989) or bovine heart mitochondrial F_1-ATPase at high (ATP) (120 µM; Vasilyeva *et al*., 1980). The inhibition of Complex V by BDE-49 was found to be mixed type as it was indicated by the Woolf-Augustinsson-Hofstee plot (shown with 20 nM BDE-49; Fig. 1C) in which the apparent K_m for ATP was 0.25 mM at 20 nM BDE-49 with an apparent V_{max} of 23 ± 2 nmol × (min × mg protein)$^{-1}$ (vs. 54 ± 2 nmol × (min × mg protein)$^{-1}$ without BDE-49). In the presence of various concentrations of BDE-49, the K_i was calculated as 6 nM (Fig. 1D; Table 1). In regards to Complex IV, kinetic analyses indicated that the inhibition of CCO by BDE-49 was noncompetitive (Fig. 1E, inset), with a K_i value of 40 nM (Table 1). No statistically significant changes in activity were identified with Complexes I, II, and III (Fig. 1F) or citrate synthase (not shown).

To gain more insight into the inhibition of Complex V by BDE-49, the oxygen uptake in State 3 was evaluated with various concentrations of BDE-49 (from 2 to 40 nM concentrations) with or without oligomycin, and the data were analyzed by means of the Yonetani-Theorell plot (Yonetani and Theorell, 1964). For each condition (i.e., with and without oligomycin), the plots of v_0/v_i (ratio of the velocities of reactions without and with oligomycin) against BDE-49 concentrations—at various concentrations of oligomycin—gave a series of intersecting straight lines, indicating simultaneous binding (mutually nonexclusive binding) of oligomycin and BDE-49 to ATPase (not shown). Thus, BDE-49 seemed to bind to sites different from catalytic and/or oligomycin-binding sites.

Effect of BDE-49 on Mitochondrial Function in NPC

To evaluate whether the observed BDE-49–mediated effects on isolated mitochondria were similar to those using intact cells, rates of oxygen uptake and coupling of electron transport to ATP synthesis were measured in NPC treated with either vehicle or BDE-49 for 2 h.

The oxygen uptake of cells supplemented sensitive to oligomycin provides a means to evaluate mitochondrial function in general and in particular the capacity to generate ATP from the electron transport chain (OXPHOS). Addition of 0.2 µM oligomycin decreased the oxygen uptake rate by 3.1-fold ($p = 4 \times 10^{-5}$), decrease that was overcome by the addition of 2 µM of the uncoupler FCCP, which increased oxygen uptake by 4.9-fold ($p = 0.03$) compared with oligomycin-inhibited rates (Fig. 2A). The addition of 0.2 nM BDE-49 (instead of that of FCCP) after oligomycin addition partly abrogated the inhibition of oxygen uptake, leading to an increase in oxygen rates of 2.9-fold ($p = 0.01$) relative to oligomycin (Fig. 2A). Higher concentrations of BDE-49 (2, 20, and 40 nM) significantly inhibited oxygen uptake in controls (by 24%, $p = 0.005$; 50%, $p = 0.01$; and 64%, $p = 0.008$, respectively; Fig. 2A). These results were a further confirmation that BDE-49, at relatively low concentrations (0.2–2 nM), acts as an uncoupler, whereas at higher (> 2 nM) concentrations, it acts as an inhibitor of the electron transport, effects consistent with those observed with isolated mitochondria. Consistent with the results obtained with intact

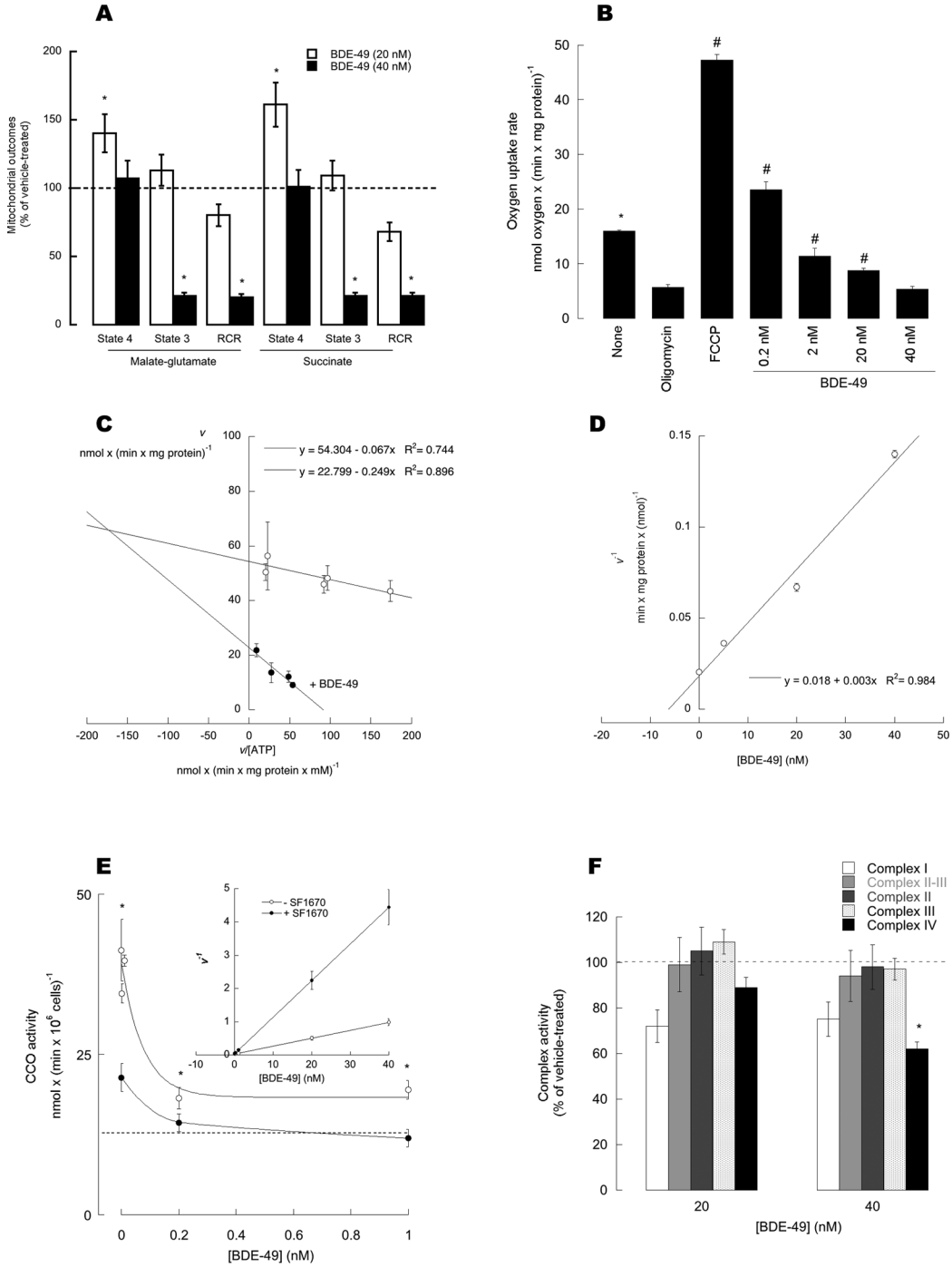

FIG. 1. Effect of BDE-49 on oxygen uptake by isolated, coupled brain mitochondria. (A) Oxygen uptake measurements and RCRs of isolated brain mitochondria after addition of 20 and 40nM BDE-49. Oxygen rates were obtained with either malate-glutamate or succinate as substrates, with 1mM ADP (State 3) or without ADP (State 4). RCR represents the ratio of State 3 to State 4 oxygen rates. Results were reported as (mean ± SEM)% of vehicle-treated mitochondria. *$p < 0.05$ versus vehicle-treated controls. (B) Oxygen uptake rates by isolated, coupled mitochondria sustained by malate-glutamate (none), supplemented with oligomycin only (oligomycin), or followed either by FCCP (FCCP) or various concentrations of BDE-49. *$p < 0.05$ versus oligomycin; Bonferroni's *post-hoc* test $p < 0.05$. (C) Representative Woolf-Augustinsson-Hofstee plot of the rates of ATPase activity versus rates divided by the substrate concentration (ATP) at 0 and 20 nM BDE-49. Calculated kinetic parameters: $V_{max} = 54 \pm 5$ nmol ATP hydrolyzed × (min × mg protein)$^{-1}$; K_m for ATP = 0.07 mM; K_i for BDE-49 = 6 nM. (D) Reciprocal of the rates of ATPase in the presence of different fixed concentrations of BDE-49. (E) Dependence of CCO activity with BDE-49 concentrations; inset: reciprocal rates versus [BDE]. (F) Complex I (open bars), Complex II and III (light grey bars), Complex II (dark gray bars), Complex III (dotted bars), and Complex IV (black bars) activities were evaluated from mitochondria treated with vehicle, 20, or 40 nM BDE-49. Activities were originally expressed as nmol × (min × mg protein)$^{-1}$ and reported as (mean ± SEM)% of vehicle-treated mitochondria. *$p < 0.05$ versus vehicle-treated controls. Oxygen rates were expressed as nmol oxygen consumed × (min × million cells)$^{-1}$. RCRu was obtained by adding oligomycin to intact cells followed by the addition of FCCP and was evaluated as the ratio between FCCP and oligomycin rates.

TABLE 1
Comparison of Inhibitory Activities of BDE-49 on Mitochondrial Complexes

	K_i (nM)	
Complex	Brain mitochondria	Neurons
I	No inhibition	No inhibition
II	No inhibition	No inhibition
III	No inhibition	No inhibition
IV	40 ± 4	0.10 ± 0.02
V	6.0 ± 0.5	(See main text)

Notes. The K_i values were calculated by unweighted, nonlinear regression fits to the median effect equation according to Martinez-Irujo *et al.* (1996). Separate measurements with MgADP ensured that BDE-49 had no effect on the coupled assay system used to evaluate ATPase activity up to 40 nM. The data were expressed as mean ± SEM.

mitochondria, BDE-49 decreased the RCRu in NPC by inhibiting State 3 oxygen uptake (Fig. 2B). Further confirmation of the role of BDE-49 as an inhibitor of the electron transport chain was obtained by following the decrease in FCCP-stimulated oxygen uptake (uncoupled respiration) by BDE-49 (Supplementary fig. 3). Of note, none of these concentrations of BDE-49 caused significant changes in cell membrane integrity or occurrence of chromatin condensation or fragmentation (Supplementary figs. 2A and B).

The activities of mitochondrial complexes (namely III, IV, and V), citrate synthase, and nonmitochondrial ATPases (i.e., resistant to the specific inhibitor oligomycin) were evaluated in NPC treated with either vehicle or BDE-49 for 2 h. The activities of Complexes III and V and citrate synthase were not changed at concentrations of 0.1–10 nM (not shown). The lack of Complex V inhibition could be explained by the small fraction of total ATPase activity that was actually oligomycin resistant (10 to 12%) and thus proving difficult to evaluate accurately any type of inhibition. Nonmitochondrial ATPase(s) activity, evaluated as oligomycin-resistant ATPase activity (such as SERCA), was lower by 20% in the presence of > 30 nM BDE-49. These experiments provided a complementary mechanism by which BDE-49 may affect calcium metabolism in addition to the one described before affecting RyR1 and ER-mitochondria calcium stores (Dingemans *et al.*, 2008; Kim *et al.*, 2011; Seo *et al.*, 2008). Complex IV activity was the only one significantly decreased (50%) at low nanomolar

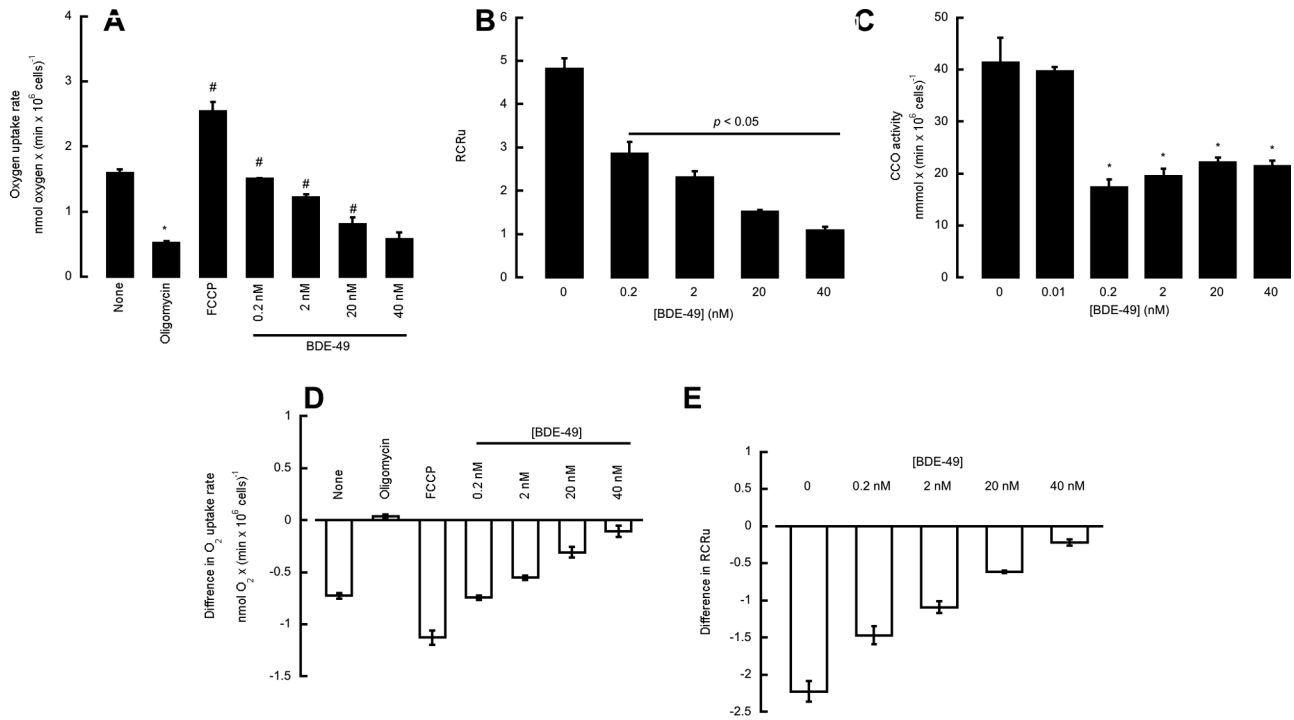

FIG. 2. Effect of BDE-49 on mitochondrial outcomes from control and PTEN-inhibited NPC. (A) Oxygen uptake in neurons in the presence of BDE-49. Oxygen rates of intact cells were determined by polarography in the presence of the indicated additions. The rates were expressed as nmol oxygen consumed × (min × million cells)$^{-1}$; (B) RCRu in neurons treated with various concentrations of BDE-49; RCRu was obtained by adding oligomycin to intact cells followed by the addition of FCCP and was evaluated as the ratio between FCCP and oligomycin rates. (C) Dependence of CCO activity with BDE-49 concentrations. (D) Effect of PTEN inhibition on oxygen uptake rates in intact neurons. The results were expressed as the difference between the rates obtained with PTEN inhibited and controls (vehicle treated). All values were significantly different from oligomycin treated ($p < 0.05$). (E) Effect of PTEN inhibition on mitochondrial coupling. The results were expressed as the difference between RCRu with PTEN inhibitor minus those from vehicle treated. RCRu is defined as the rate of oxygen uptake in State 3u (with substrate and FCCP) divided by that in oligomycin-inhibited State 4. Values obtained with BDE-49 were significantly different from vehicle treated with $p < 0.05$.

concentrations of BDE-49 ($p < 0.05$; Fig. 2C). Kinetic analyses indicated that 0.1 nM BDE-49 was required to inhibit 50% of Complex IV activity. This parameter compared with that obtained with isolated mitochondria (Table 1) was 400-fold higher, suggesting that BDE-49 may have accumulated in mitochondria within the cells to reach the inhibitory concentration. The fold of accumulation compared favorably to that reported for BDE-47 in mouse CGN cells (500-fold at an applied concentration of 0.01 µM; Huang *et al*., 2010).

PTEN-Deficient Background Enhances the Deleterious Effect of BDE-49 on Mitochondrial Function

To test how a background associated with abnormal social and repetitive behavior, such as that observed in PTEN deficiency, influences the toxicity of BDE-49, PTEN activity was selectively inhibited in NPC by treatment with the inhibitor SF1670 (Li *et al*., 2011). The inhibition of PTEN was evaluated by the increase in pAkt as described before (Napoli *et al*., 2012) and shown in Supplementary figure 4, given that PTEN is a negative regulator of the PI3K/Akt pathway (Li *et al*., 2011).

PTEN inhibition resulted in decreases in Complex IV activity (by 50%; $p = 0.02$) because PTEN deficiency, via downregulation of p53 and subsequently that of the p53-downstrean target SCO2, affects Complex IV activity as observed in the brain of PTEN haploinsufficient mice (Napoli *et al*., 2012). Rates of oxygen uptake and coupling of electron transport to ATP synthesis were measured in controls and PTEN-inhibited cells in the presence of various concentrations of BDE-49 (Figs. 2D and E). Addition of 0.2, 2, 20, and 40 nM BDE-49 to FCCP-stimulated cells resulted in an oxygen uptake inhibition of, respectively, 42, 52, 65, and 72%. PTEN-inhibited cells showed a decrease in both glucose-supported oxygen uptake and coupling by 46% ($p = 0.0006$ and $p = 0.01$, respectively; Figs. 2D and E). Addition of 2, 20, and 40 nM BDE-49 further decreased the State 3u oxygen uptake by an extra 24% ($p = 0.0001$), 43% ($p = 0.04$), and 46% ($p = 0.04$), resulting in a final inhibition of 70, 89, and 92% (Fig. 2D). Parallel decreases in coupling were observed as well (Fig. 2E). The inhibitory effect of BDE-49 on FCCP-stimulated oxygen uptake was evaluated in control and PTEN-inhibited NPC (Supplementary fig. 3). Addition of 0.2, 2, 20, and 40 nM BDE-49 to FCCP-stimulated cells resulted in an oxygen uptake inhibition of, respectively, 42, 52, 65, and 72%. Pretreatment of NPC with SF1670, followed by addition of the same BDE-49 concentrations, led to inhibitions equal to 70% (0.2 nM), 75% (2 nM), and 80% (at 20 and 40 nM). These results (along with the lack of changes in cell membrane integrity and chromatin fragmentation and/or condensation; Supplementary figs. 2A and B) were consistent with those observed with isolated brain mitochondria (Fig. 1).

Although the activity of Complex IV in PTEN-inhibited cells was reduced by half, addition of BDE-49 at concentrations equal to its K_i resulted in an additional 20% inhibition (for a total of 70%; $p = 0.05$). Although an additional 20% inhibition may not seem quantitatively and/or biologically relevant, enzymatic activity thresholds for cells in culture are set at 20% (for major criteria) and 30% (for minor criteria) of control activities for diagnosing mitochondrial respiratory chain diseases (Bernier *et al*., 2002).

Altered Mitochondrial Distribution and Morphology in NPC Treated With BDE-49 in a PTEN-Deficient Background

Differences in the distribution and morphology of mitochondria in NPC exposed to BDE-49 were evaluated by using MitoTracker Deep Red, dye that stains polarized mitochondria (Poot *et al*., 1996) (Figs. 3A and B). In vehicle-treated cells, mitochondria were distributed throughout the cell (Fig. 3A) and organized as an extended network of tubular structures (Fig. 3B) (Liot *et al*., 2009). However, this network in BDE-49–treated cells appeared disrupted, significantly more fragmented and with a different distribution pattern, with the majority of mitochondria distributed around the perinuclear region of the cell (Figs. 3A and B). Furthermore, measurement of the total Mitotracker fluorescent signal showed a 1.5-fold increase in BDE-49–treated mitochondria (relative to vehicle treated, $p < 0.01$; Fig. 3B; Supplementary fig. 5), likely attributed to hyperpolarization of the mitochondrial membrane caused by the inhibitory effect of BDE-49 on ETC. In a PTEN-deficient background, the distribution of mitochondria upon addition of BDE-49 was still perinuclear, as observed with BDE-49 only, with a 1.7-fold increase of Mitotracker fluorescent intensity relative to vehicle-treated cells ($p < 0.001$; Fig. 3B; Supplementary fig. 5) and a 1.2-fold increase versus BDE-49 alone ($p < 0.05$; Supplementary fig. 5). Thus, the effects of a PTEN-deficient background and that of BDE-49 are synergistic, resulting in more polarized mitochondria, increased fragmentation, and disrupted network.

The occurrence of smaller, more fragmented mitochondria in BDE-49–treated cells (regardless of a PTEN-deficient background) suggested the activation of a selective autophagy or mitophagy responsible for the removal of damaged mitochondria (Ashrafi and Schwarz, 2013). This process initiated by oxidative stress–mediated damage leads to the activation of dynamin-related protein 1 (Drp1), whose polymerization promotes mitochondrial fission, segregating damaged mitochondria versus undamaged ones for ultimate elimination from the cell (Elgass *et al*., 2013). We reasoned that as Akt overexpression or PTEN deficiency inhibits mitophagy (Napoli *et al*., 2012; Zhou *et al*., 2009), putative increases in oxidative stress originated from BDE-49 inhibition of ETC could antagonize and overcome this potent signal, resulting in activation of clearance of damaged mitochondria. To test this hypothesis, we evaluated three markers of oxidative stress, i.e., increases in Tyr nitration of ATPase beta subunit (Fujisawa *et al*., 2009; Haynes *et al*., 2010), mtDNA copy number, and mtDNA deletions (Lee and Wei, 2005). Treatment of NPC with 40 nM BDE-49 resulted in an increased Tyr nitration of ATPase beta subunit (twofold of controls; $p = 0.024$; Fig. 4A), regardless of the PTEN background (Fig. 4A). The mtDNA copy number in NPC

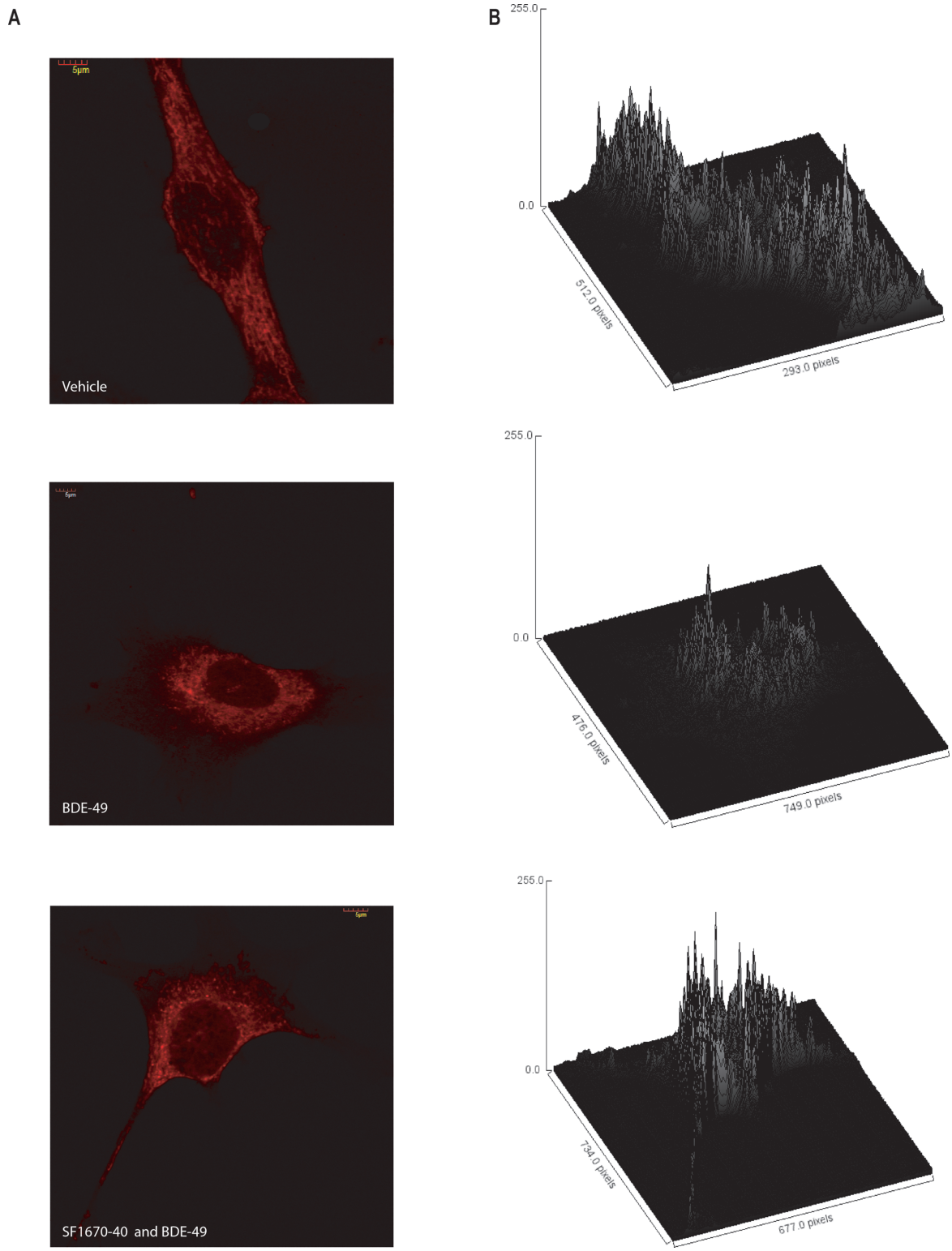

FIG. 3. Mitochondrial distribution and morphology in NPC in the presence of BDE-49 and in a PTEN-deficient background. (A) Confocal images of NPC probed with MitoTracker Deep Red FM. Cells were plated onto polylysine-coated coverslips and stained as described in the Materials and Methods section. Images were taken with an Olympus FV1000 laser scanning confocal microscope at 60× magnification and zooms variable between 2.0 and 3.0. The images shown were representative of at least 100 cells. (B) Three-dimensional surface plot of mitochondrial distribution in NPC treated with vehicle, 40 nM BDE-49, and BDE-49 and 3 nM of the PTEN inhibitor SF1670. Surface plots were computed with Image J software and displayed as a three-dimensional graph of the intensities of pixels of the confocal images shown in (A).

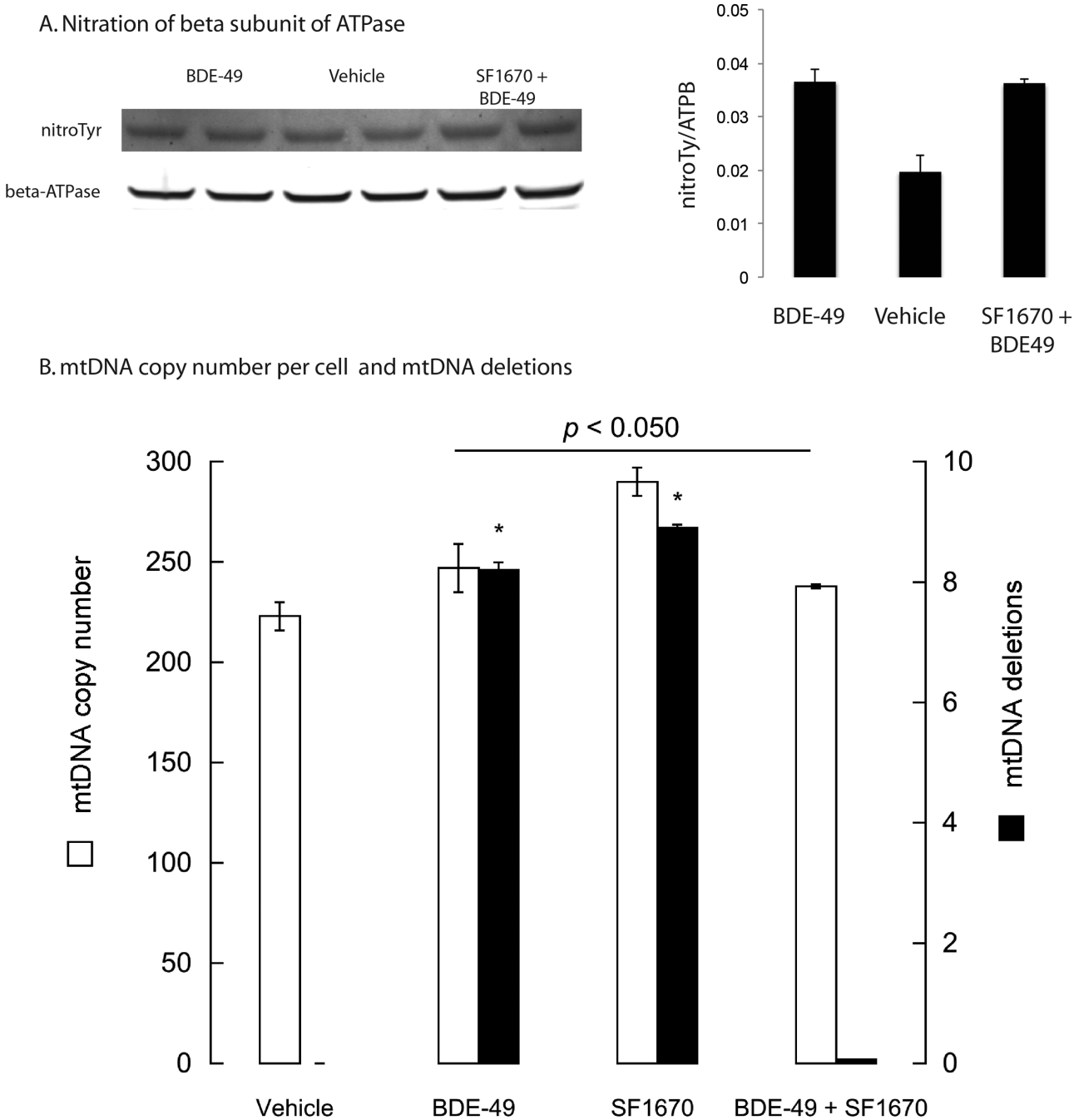

FIG. 4. Evaluation of oxidative/nitrative stress in BDE-49–treated NPC. (A) Nitration levels of the beta subunit of mitochondrial ATPase in NPC treated with vehicle, BDE-49, and BDE-49 and the PTEN inhibitor SF1670. Western blots were performed as described in the Materials and Methods section. Nitrotyrosine fluorescent intensities were normalized by those of the beta subunit of mitochondrial ATPase. *$p < 0.05$ versus vehicle treated. (B) Mitochondrial DNA copy number (mtDNA) and mtDNA deletions in vehicle-, BDE-49–, SF1670-, and BD49 plus SF1670-treated NPC. Details on the primers and PCR conditions used are reported in the Supplementary methods. The p value at the top of the line corresponds to mtDNA copy number of all treatments versus vehicle treated, whereas the asterisk corresponds to mtDNA deletions versus vehicle treated. mtDNA deletions were expressed as percentage of vehicle values.

treated with BDE-49 only, SF1670 only, and both treatments was higher than vehicle treated (by 11, 30, and 7%; $p < 0.05$; Fig. 4B). These data were consistent with previous reports in which increases in mtDNA copy number and reactive oxygen species (ROS) production were not accompanied by increases in OXPHOS (Giulivi *et al.*, 2010; Lee and Wei, 2005; Lee *et al.*, 2002; Liu *et al.*, 2003). The accumulation of mtDNA deletions was higher in BDE-49–treated cells and PTEN-inhibited cells (8 and 9%, respectively) than controls, whereas the addition of BDE-49 to PTEN-inhibited cells resulted in lower mtDNA

deletions (0.1%; Fig. 4B). These results were suggestive that BDE-49 exposure, via increased oxidative stress, may enhance mitophagy and overcome the antagonistic effect of PTEN deficiency in this process, resulting in no significant changes in nitration of ATPase beta subunit, lower mtDNA copy number, and decreased accumulation of mtDNA deletions compared with BDE-49-only treatment.

DISCUSSION

In this study, BDE-49 acted as an uncoupler of electron transport and ATP synthesis when added to isolated, coupled brain mitochondria and NPC at low concentrations (< 0.1 nM), whereas at higher concentrations (≥ 20 nM), it acted as an inhibitor of Complexes IV and V, disrupted mitochondrial morphology and polarization, and increased oxidative/nitrative stress (as judged by increased Tyr nitration in ATPase, mtDNA copy number and mtDNA deletions). Based on the K_i for CCO in mitochondria and cells, the accumulation of BDE-49 in neurons was estimated as 400-fold, similar to those reported for other PBDEs (two or more orders of magnitude; Huang *et al*., 2010; Mundy *et al*., 2004). These concentrations of BDE-49 that altered mitochondrial outcomes could be regarded as biologically relevant for they could be easily reached with the reported plasma concentrations of BDE-47 of children living in Mexico and California (0.07–1.8 nM; Eskenazi *et al*., 2011; Hertz-Picciotto *et al*., 2011) and considering that a significant percentage of PBDE accumulates in mitochondria (30% of total BDE-47 added to CGN neurons; Huang *et al*., 2010). Uncoupling has been also reported for a similar congener, BDE-47, using zebrafish mitochondria along with an inhibitory effect on succinate dehydrogenase activity (van Boxtel *et al*., 2008). Although uncoupling and inhibition of electron transport are distinct processes, both converge on the same outcome, i.e., a disrupted energy production that could be enhanced or potentiated by an increased production of ROS.

Typical uncoupling is usually observed in situations in which the rate of oxygen uptake in State 4 is increased to levels comparable to those of State 3. The significant decrease in RCR resulting from higher State 4 oxygen uptake rate and the release of oligomycin-inhibited oxygen uptake confirm the role of BDE-49 as an uncoupler of OXPHOS at relatively low concentrations. Many hypotheses have been advanced to explain the mechanism by which compounds can uncouple OXPHOS in mitochondria. All those compounds are characterized by being lipid soluble, having a dissociable proton, and a structure permitting a large charge delocalization (Cunarro and Weiner, 1975; van Dam and Slater, 1967; Weinbach and Garbus, 1969). Thus, given that BDE-49 is highly lipophilic (log P 6.89 and Clog P 7.23) but does not have an ionizable hydroxyl group, it is possible that the uncoupling effect is caused by incorporation of BDE-49 to the membrane disrupting its assembly (especially considering the lack of planarity; Fig. 5) or a direct effect on ATPase favoring dissipation of the proton gradient (Terada, 1981). This dual effect of BDE-49, i.e., acting as an uncoupler at relatively low concentrations while becoming an inhibitor of electron transport at higher ones, has also been observed with other uncouplers of OXPHOS (Chappell, 1964; Goldsby and Heytler, 1963; Heytler, 1963).

Alternatively, BDE-49 may have an effect on the activity of uncoupling proteins (UCP). Three of the five human UCP homologues, namely, UCP2, UCP4, and UCP5, are located in the central nervous system (Naert *et al*., 2007), and in our murine cell model, we observed a significant gene expression of UCP2. It could be hypothesized that (1) BDE-49 at low concentrations may have an effect on cardiolipin packing, increasing indirectly the activity of UCP2 (Hoang *et al*., 2012) favoring uncoupling of electron transport and ATP synthesis, and (2) this uncoupling may serve as an attempt to decrease/suppress ROS production by mitochondria, suggesting a protective mechanism against oxidative stress as suggested by others (Andrews *et al*., 2005; Echtay, 2007; Krauss *et al*., 2005). A direct effect of BDE-49 on UCP2 activity seems unlikely given the differences in chemical structure between this compound and fatty acids. However, increased mitochondrial oxidative/nitrative stress in NPC at (BDE-49) > 20 nM suggests that the putative effect of BDE-49 on UCP is not observed at these higher concentrations as supported by the higher polarization of mitochondria (as observed by MitoTracker staining).

The inhibition of electron transport by BDE-49 was exerted at the level of Complexes V and IV. In regards to the inhibition of Complex V activity, the K_i of BDE-49 (0.33 nmol/mg protein) was in the range of those reported for other inhibitors of ATPase (for > 90% inhibition, aurovertin B 0.4 nmol/mg protein, oligomycin 0.6 nmol/mg protein). This finding, together with the K_i values reported in Table 1, suggested that BDE-49 was a more potent inhibitor of Complex V than IV; however, the similar pattern of inhibition of both State 3 oxygen uptake by intact mitochondria and Complex IV activity by BDE-49, and the lack of correspondence with Complex V suggest that phosphorylating mitochondria were more sensitive to the BDE-49–mediated inhibition of the terminal oxidase over that of Complex V. One possible explanation is to consider that BDE-49 altered the higher K_m for ATP in Complex V. This K_m represents the binding of ATP to noncatalytic sites, which accelerates catalysis, presumably by promoting release of inhibitory MgADP from a catalytic site (Jault and Allison, 1993). The amount and composition of the noncatalytic-site nucleotides affect both the formation and the ATP-dependent discharge of the Mg^{2+} and ADP inhibition (Milgrom *et al*., 1991). Although F_1 can hydrolyze ATP without ATP binding at noncatalytic sites, the steady-state rate is increased by such binding (Murataliev and Boyer, 1992). In our case, BDE-49 seems to affect the binding of ATP at the noncatalytic sites, decreasing the affinity for ATP; thus, when loading of noncatalytic sites is accomplished with free ATP, the lower affinity of noncatalytic sites in BDE-49–treated Complex V might fill less with ATP on introducing the enzyme to the assay medium, resulting in lower initial rate of hydrolysis.

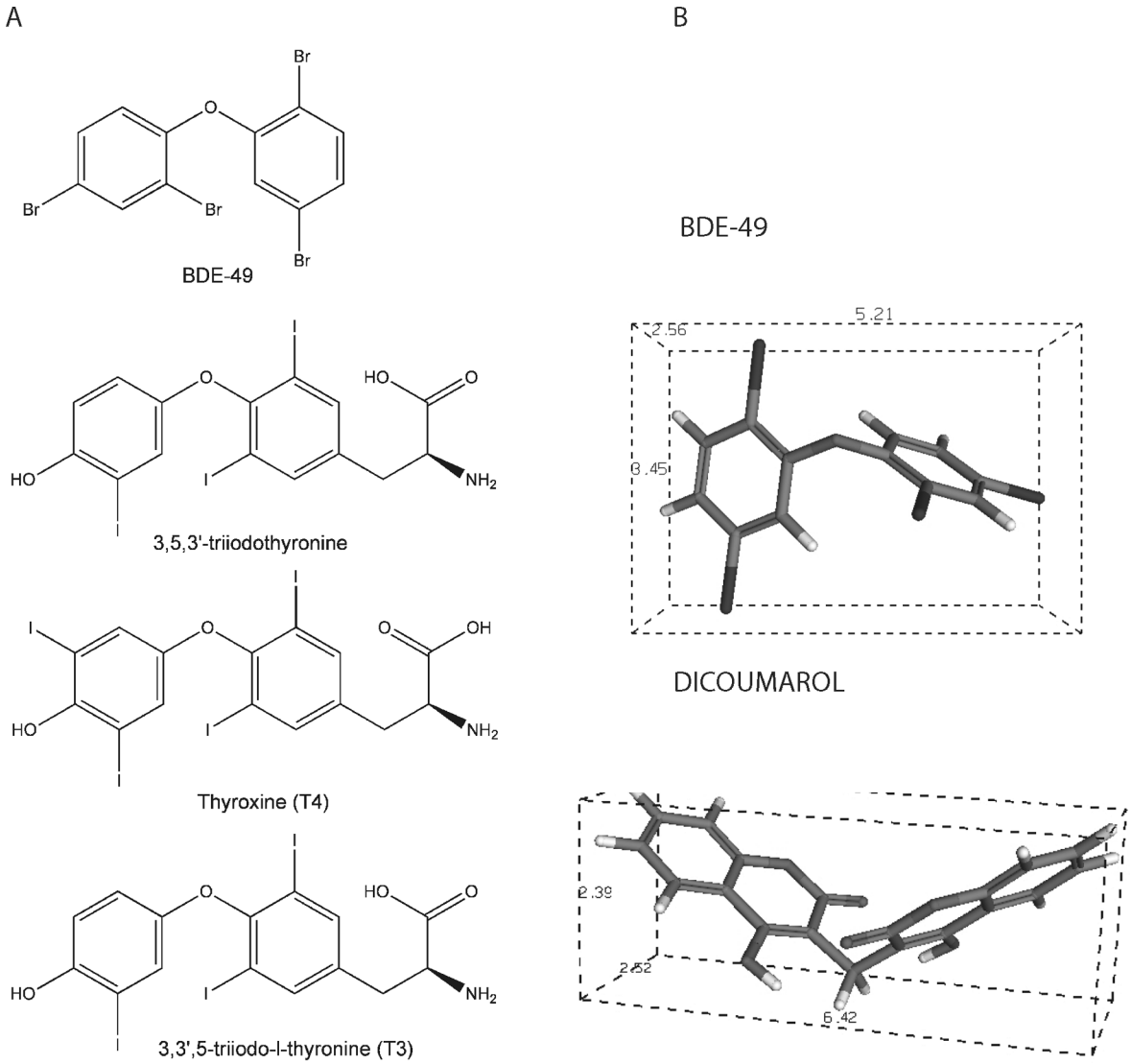

FIG. 5. BDE-49, iodothyronines, and dicoumarol chemical structures. (A) Chemical structures of tri- and tetraiodothyronines and BDE-49. (B) Three-dimensional structures of BDE-49 and dicoumarol (structures obtained with CS ChemOffice and visualized using PC3DView).

The fact that oligomycin and BDE-49 bind simultaneously to ATPase suggests either independent binding to two different sites or binding to two sites in close proximity modifying BDE-49 binding site. Although independent inhibitor binding would suggest that the sites do not interact at all, calculations for the mutual influence factor gamma from the Yonetani-Theorell plots indicated that oligomycin might lock the F_1-ATPase conformation disfavoring the binding of the subsequent inhibitor (BDE-49), even if they bind to unique sites. Furthermore, the fact that BDE-49 acted as a mixed-type inhibitor confirms the binding of this PBDE congener to a site different from the catalytic site of ATP on the beta subunit.

Although the inhibition of Complex IV by BDE-49 would require further investigation, we could propose that direct binding of BDE-49 to Complex IV subunits may elicit critical conformational changes considering that the chemical structure of this compound is similar to that of di- and tri-iodothyronines, compounds that bind and modify CCO activity (Goglia *et al.*, 1994). Alternatively, BDE-49 may affect either the binding of cytochrome *c* to the docking site on Complex IV or the membrane structure/packing by intercalating in the lipid bilayer as it has been proposed for another uncoupler, dicoumarol (Fig. 3; Wilson and Merz, 1969).

The importance at considering genetic backgrounds that may confer heightened susceptibility to the exposure of an environmental factor is evidenced in our study in which PTEN deficiency enhanced the already present BDE-49–mediated MD. If perinatal PBDE exposure were one of the precipitating factors in the concept of "second-hit stress" (i.e., BDE-49 after PTEN inhibition), then the severity of the inherited background (e.g., PTEN haploinsufficiency vs. null or KO) in a particular tissue (e.g., neurons) would set the

initial bioenergetic capacity during perinatal period and thus the relative severity of the disease at birth. Individuals with initially high mitochondrial bioenergetic capacities would require multiple exposures or a combination of triggers to cross-expression thresholds and thus remain functional until late in life, whereas individuals who inherit significantly deleterious backgrounds would start at a lower initial capacity and require fewer exposures or combination of them to have the same effect and would develop symptoms at birth or during childhood. In this last setting, the relatively mild 20–30% PBDE-induced bioenergetic decline on top of the original one (caused by PTEN deficiency or by partial OXPHOS defects (Offit, 2008)), which could be seen as being not physiologically relevant, reached the energy threshold for synaptic mitochondria (major changes in OXPHOS occur with decreases in CCO activity of 70% (Davey *et al*., 1998)), suggesting that this "second-hit stress" might induce the expression of a phenotype considering that brain is a highly aerobic organ and heavily dependent on OXPHOS for ATP supply.

More importantly, BDE-49–mediated decreases in Complex IV activity become relevant in clinical cases with preexisting Complex IV deficiencies and/or mutations in CCO assembly genes (deficiencies implicated in several psychiatric and neurological disorders, including autism; Giulivi *et al*., 2010; Joost *et al*., 2010; Ohta and Ohsawa, 2006; Oliveira *et al*., 2005; Papadopoulou *et al*., 1999; Tulinius *et al*., 2003), whereas decreases in F_1F_o-ATPase seem to play a crucial role in the pathophysiology of several human disorders, including ischemia-reperfusion injury, cancer, cholesterol homoeostasis, and neurological disorders (Finsterer, 2008; Giulivi *et al*., 2010; Thyagarajan *et al*., 1995; Verny *et al*., 2011).

Although our study was performed with a biologically relevant but acute doses of BDE-49, it could be envisioned as a model of gene-environment interaction over chronic exposures to BDE-49 with the potential to affect neurodevelopment considering that perinatal periods are the most vulnerable for PBDE exposure (Lunder *et al*., 2010) and that children accumulate more PBDEs than adults when sharing the same environment (ΣPBDEs in children aged 1.4–4 years were 2.8-times that of mothers; Lunder *et al*., 2010). Furthermore, it has been shown that children with higher concentrations of BDEs 47, 99, or 100 in cord blood scored lower on tests of mental and physical development at 12–48 and 72 months (Herbstman *et al*., 2010).

Considering the dependency of brain for mitochondrial ATP required to maintain neuronal growth and development, exposure to one of the PBDE congeners, i.e., BDE-49, without necessarily being one of the most abundant, may result in energy deficits that may contribute to learning and cognitive deficiencies. The impact of this exposure may become more relevant in vulnerable populations, such as young children in general, and especially among those with a genetic background that confers increased susceptibility to this exposure.

SUPPLEMENTARY DATA

Supplementary data are available online at http://toxsci.oxfordjournals.org/.

FUNDING

Autism Speaks Foundation (2344); partially by National Institutes of Environmental Health (R01-ES012691, R01-ES020392).

ACKNOWLEDGMENTS

We thank the excellent technical assistance of Dr Robert Schoenfeld with cell culture.

REFERENCES

Andrews, Z. B., Diano, S., and Horvath, T. L. (2005). Mitochondrial uncoupling proteins in the CNS: In support of function and survival. *Nat. Rev. Neurosci.* **6,** 829–840.

Ashrafi, G., and Schwarz, T. L. (2013). The pathways of mitophagy for quality control and clearance of mitochondria. *Cell Death Differ.* **20,** 31–42.

Baio, J. (2012). Prevalence of autism spectrum disorders--Autism and Developmental Disabilities Monitoring Network, 14 sites, United States, 2008. *MMWR Surveill. Summ.* **61,** 1–19.

Bernier, F. P., Boneh, A., Dennett, X., Chow, C. W., Cleary, M. A., and Thorburn, D. R. (2002). Diagnostic criteria for respiratory chain disorders in adults and children. *Neurology* **59,** 1406–1411.

Betts, K. S. (2002). Rapidly rising PBDE levels in North America. *Environ. Sci. Technol.* **36,** 50A–52A.

Birnbaum, L. S., and Staskal, D. F. (2004). Brominated flame retardants: Cause for concern? *Environ. Health Perspect.* **112,** 9–17.

Branchi, I., Capone, F., Alleva, E., and Costa, L. G. (2003). Polybrominated diphenyl ethers: Neurobehavioral effects following developmental exposure. *Neurotoxicology* **24,** 449–462.

Browne, E. P., Stapleton, H. M., Kelly, S. M., Tilton, S. C., and Gallagher, E. P. (2009). In vitro hepatic metabolism of 2,2',4,4',5-pentabromodiphenyl ether (BDE 99) in Chinook salmon (Onchorhynchus tshawytscha). *Aquat. Toxicol.* **92,** 281–287.

Bruel-Jungerman, E., Davis, S., and Laroche, S. (2007). Brain plasticity mechanisms and memory: A party of four. *Neuroscientist* **13,** 492–505.

Butler, M. G., Dasouki, M. J., Zhou, X. P., Talebizadeh, Z., Brown, M., Takahashi, T. N., Miles, J. H., Wang, C. H., Stratton, R., Pilarski, R., *et al.* (2005). Subset of individuals with autism spectrum disorders and extreme macrocephaly associated with germline PTEN tumour suppressor gene mutations. *J. Med. Genet.* **42,** 318–321.

Buxbaum, J. D., Cai, G., Chaste, P., Nygren, G., Goldsmith, J., Reichert, J., Anckarsäter, H., Rastam, M., Smith, C. J., Silverman, J. M., *et al.* (2007). Mutation screening of the PTEN gene in patients with autism spectrum disorders and macrocephaly. *Am. J. Med. Genet. B Neuropsychiatr. Genet.* **144B,** 484–491.

Chappell, J. B. (1964). The effects of 2,4-dinitrophenol on mitochondrial oxidations. *Biochem. J.* **90,** 237–248.

Coburn, C. G., Currás-Collazo, M. C., and Kodavanti, P. R. (2008). In vitro effects of environmentally relevant polybrominated diphenyl ether (PBDE) congeners on calcium buffering mechanisms in rat brain. *Neurochem. Res.* **33,** 355–364.

Costa, L. G., Giordano, G., Tagliaferri, S., Caglieri, A., and Mutti, A. (2008). Polybrominated diphenyl ether (PBDE) flame retardants: Environmental contamination, human body burden and potential adverse health effects. *Acta Biomed.* **79,** 172–183.

Cunarro, J., and Weiner, M. W. (1975). Mechanism of action of agents which uncouple oxidative phosphorylation: Direct correlation between proton-carrying and respiratory-releasing properties using rat liver mitochondria. *Biochim. Biophys. Acta* **387,** 234–240.

Darnerud, P. O. (2003). Toxic effects of brominated flame retardants in man and in wildlife. *Environ. Int.* **29,** 841–853.

Darnerud, P. O., Eriksen, G. S., Jóhannesson, T., Larsen, P. B., and Viluksela, M. (2001). Polybrominated diphenyl ethers: Occurrence, dietary exposure, and toxicology. *Environ. Health Perspect.* **109**(Suppl. 1), 49–68.

Davey, G. P., Peuchen, S., and Clark, J. B. (1998). Energy thresholds in brain mitochondria. Potential involvement in neurodegeneration. *J. Biol. Chem.* **273,** 12753–12757.

Davis, J. A., Hetzel, F., Oram, J. J., and McKee, L. J. (2007). Polychlorinated biphenyls (PCBs) in San Francisco Bay. *Environ. Res.* **105,** 67–86.

Di Martino, A., Kelly, C., Grzadzinski, R., Zuo, X. N., Mennes, M., Mairena, M. A., Lord, C., Castellanos, F. X., and Milham, M. P. (2011). Aberrant striatal functional connectivity in children with autism. *Biol. Psychiatry* **69,** 847–856.

Dingemans, M. M., de Groot, A., van Kleef, R. G., Bergman, A., van den Berg, M., Vijverberg, H. P., and Westerink, R. H. (2008). Hydroxylation increases the neurotoxic potential of BDE-47 to affect exocytosis and calcium homeostasis in PC12 cells. *Environ. Health Perspect.* **116,** 637–643.

Dingemans, M. M., Heusinkveld, H. J., Bergman, A., van den Berg, M., and Westerink, R. H. (2010a). Bromination pattern of hydroxylated metabolites of BDE-47 affects their potency to release calcium from intracellular stores in PC12 cells. *Environ. Health Perspect.* **118,** 519–525.

Dingemans, M. M., van den Berg, M., Bergman, A., and Westerink, R. H. (2010b). Calcium-related processes involved in the inhibition of depolarization-evoked calcium increase by hydroxylated PBDEs in PC12 cells. *Toxicol. Sci.* **114,** 302–309.

Dingemans, M. M., van den Berg, M., and Westerink, R. H. (2011). Neurotoxicity of brominated flame retardants: (In)direct effects of parent and hydroxylated polybrominated diphenyl ethers on the (developing) nervous system. *Environ. Health Perspect.* **119,** 900–907.

Dobbing, J., and Sands, J. (1979). Comparative aspects of the brain growth spurt. *Early Hum. Dev.* **3,** 79–83.

Echtay, K. S. (2007). Mitochondrial uncoupling proteins–what is their physiological role? *Free Radic. Biol. Med.* **43,** 1351–1371.

Elfering, S. L., Haynes, V. L., Traaseth, N. J., Ettl, A., and Giulivi, C. (2004). Aspects, mechanism, and biological relevance of mitochondrial protein nitration sustained by mitochondrial nitric oxide synthase. *Am. J. Physiol. Heart Circ. Physiol.* **286,** H22–H29.

Elgass, K., Pakay, J., Ryan, M. T., and Palmer, C. S. (2013). Recent advances into the understanding of mitochondrial fission. *Biochim. Biophys. Acta* **1833,** 150–161.

Eriksson, P. S., Perfilieva, E., Björk-Eriksson, T., Alborn, A. M., Nordborg, C., Peterson, D. A., and Gage, F. H. (1998). Neurogenesis in the adult human hippocampus. *Nat. Med.* **4,** 1313–1317.

Eskenazi, B., Fenster, L., Castorina, R., Marks, A. R., Sjödin, A., Rosas, L. G., Holland, N., Guerra, A. G., Lopez-Carillo, L., and Bradman, A. (2011). A comparison of PBDE serum concentrations in Mexican and Mexican-American children living in California. *Environ. Health Perspect.* **119,** 1442–1448.

Estabrook, R. W. (1967). Mitochondrial respiratory control and the polarographic measurement of ADP:O ratios. *Meth. Enzymol.* **10,** 41–47.

Finsterer, J. (2008). Leigh and Leigh-like syndrome in children and adults. *Pediatr. Neurol.* **39,** 223–235.

Flegal, A. R., Brown, C. L., Squire, S., Ross, J. R., Scelfo, G. M., and Hibdon, S. (2007). Spatial and temporal variations in silver contamination and toxicity in San Francisco Bay. *Environ. Res.* **105,** 34–52.

Fraser, M. M., Bayazitov, I. T., Zakharenko, S. S., and Baker, S. J. (2008). Phosphatase and tensin homolog, deleted on chromosome 10 deficiency in brain causes defects in synaptic structure, transmission and plasticity, and myelination abnormalities. *Neuroscience* **151,** 476–488.

Fujisawa, Y., Kato, K., and Giulivi, C. (2009). Nitration of tyrosine residues 368 and 345 in the beta-subunit elicits FoF1-ATPase activity loss. *Biochem. J.* **423,** 219–231.

Garcia-Cao, I., Song, M. S., Hobbs, R. M., Laurent, G., Giorgi, C., de Boer, V. C., Anastasiou, D., Ito, K., Sasaki, A. T., Rameh, L., *et al.* (2012). Systemic elevation of PTEN induces a tumor-suppressive metabolic state. *Cell* **149,** 49–62.

Giulivi, C., Zhang, Y. F., Omanska-Klusek, A., Ross-Inta, C., Wong, S., Hertz-Picciotto, I., Tassone, F., and Pessah, I. N. (2010). Mitochondrial dysfunction in autism. *JAMA* **304,** 2389–2396.

Goffin, A., Hoefsloot, L. H., Bosgoed, E., Swillen, A., and Fryns, J. P. (2001). PTEN mutation in a family with Cowden syndrome and autism. *Am. J. Med. Genet.* **105,** 521–524.

Goglia, F., Lanni, A., Barth, J., and Kadenbach, B. (1994). Interaction of diiodothyronines with isolated cytochrome c oxidase. *FEBS Lett.* **346,** 295–298.

Goldsby, R. A., and Heytler, P. G. (1963). Uncoupling of oxidative phosphorylation by carbonyl cyanide phenylhydrazones. Ii. Effects of carbonyl cyanide m-chlorophenylhydrazone on mitochondrial respiration. *Biochemistry* **2,** 1142–1147.

Gottlieb, R. A., and Carreira, R. S. (2010). Autophagy in health and disease. 5. Mitophagy as a way of life. *Am. J. Physiol., Cell Physiol.* **299,** C203–C210.

Haynes, V., Traaseth, N. J., Elfering, S., Fujisawa, Y., and Giulivi, C. (2010). Nitration of specific tyrosines in FoF1 ATP synthase and activity loss in aging. *Am. J. Physiol. Endocrinol. Metab.* **298,** E978–E987.

Herbstman, J. B., Sjödin, A., Kurzon, M., Lederman, S. A., Jones, R. S., Rauh, V., Needham, L. L., Tang, D., Niedzwiecki, M., Wang, R. Y., *et al.* (2010). Prenatal exposure to PBDEs and neurodevelopment. *Environ. Health Perspect.* **118,** 712–719.

Herman, G. E., Butter, E., Enrile, B., Pastore, M., Prior, T. W., and Sommer, A. (2007). Increasing knowledge of PTEN germline mutations: Two additional patients with autism and macrocephaly. *Am. J. Med. Genet. A* **143,** 589–593.

Hertz-Picciotto, I., Bergman, A., Fängström, B., Rose, M., Krakowiak, P., Pessah, I., Hansen, R., and Bennett, D. H. (2011). Polybrominated diphenyl ethers in relation to autism and developmental delay: A case-control study. *Environ. Health* **10,** 1.

Hertz-Picciotto, I., and Delwiche, L. (2009). The rise in autism and the role of age at diagnosis. *Epidemiology* **20,** 84–90.

Heytler, P. G. (1963). Uncoupling of oxidative phosphorylation by carbonyl cyanide phenylhydrazones. I. Some characteristics of m-Cl-CCP action on mitochondria and chloroplasts. *Biochemistry* **2,** 357–361.

Hoang, T., Smith, M. D., and Jelokhani-Niaraki, M. (2012). Toward understanding the mechanism of ion transport activity of neuronal uncoupling proteins UCP2, UCP4, and UCP5. *Biochemistry* **51,** 4004–4014.

Hu, X., Hu, D., and Xu, Y. (2009). Effects of tetrabrominated diphenyl ether and hexabromocyclododecanes in single and complex exposure to hepatoma HepG2 cells. *Environ. Toxicol. Pharmacol.* **27,** 327–337.

Huang, S. C., Giordano, G., and Costa, L. G. (2010). Comparative cytotoxicity and intracellular accumulation of five polybrominated diphenyl ether congeners in mouse cerebellar granule neurons. *Toxicol. Sci.* **114,** 124–132.

Jault, J. M., and Allison, W. S. (1993). Slow binding of ATP to noncatalytic nucleotide binding sites which accelerates catalysis is responsible for apparent negative cooperativity exhibited by the bovine mitochondrial F1-ATPase. *J. Biol. Chem.* **268,** 1558–1566.

Joost, K., Rodenburg, R., Piirsoo, A., van den Heuvel, B., Zordania, R., and Ounap, K. (2010). A novel mutation in the SCO2 gene in a neonate with early-onset cardioencephalomyopathy. *Pediatr. Neurol.* **42,** 227–230.

Kim, K. H., Bose, D. D., Ghogha, A., Riehl, J., Zhang, R., Barnhart, C. D., Lein, P. J., and Pessah, I. N. (2011). Para- and ortho-substitutions are key determinants of polybrominated diphenyl ether activity toward ryanodine receptors and neurotoxicity. *Environ. Health Perspect.* **119,** 519–526.

Kodavanti, P. R., and Ward, T. R. (2005). Differential effects of commercial polybrominated diphenyl ether and polychlorinated biphenyl mixtures on intracellular signaling in rat brain in vitro. *Toxicol. Sci.* **85,** 952–962.

Krauss, S., Zhang, C. Y., and Lowell, B. B. (2005). The mitochondrial uncoupling-protein homologues. *Nat. Rev. Mol. Cell Biol.* **6,** 248–261.

Kwon, C. H., Luikart, B. W., Powell, C. M., Zhou, J., Matheny, S. A., Zhang, W., Li, Y., Baker, S. J., and Parada, L. F. (2006). Pten regulates neuronal arborization and social interaction in mice. *Neuron* **50,** 377–388.

Langen, M., Schnack, H. G., Nederveen, H., Bos, D., Lahuis, B. E., de Jonge, M. V., van Engeland, H., and Durston, S. (2009). Changes in the developmental trajectories of striatum in autism. *Biol. Psychiatry* **66,** 327–333.

Lee, H. C., and Wei, Y. H. (2005). Mitochondrial biogenesis and mitochondrial DNA maintenance of mammalian cells under oxidative stress. *Int. J. Biochem. Cell Biol.* **37,** 822–834.

Lee, H. C., Yin, P. H., Chi, C. W., and Wei, Y. H. (2002). Increase in mitochondrial mass in human fibroblasts under oxidative stress and during replicative cell senescence. *J. Biomed. Sci.* **9**(6 Pt 1), 517–526.

Lee, J., Giordano, S., and Zhang, J. (2012). Autophagy, mitochondria and oxidative stress: Cross-talk and redox signalling. *Biochem. J.* **441,** 523–540.

Li, Y., Prasad, A., Jia, Y., Roy, S. G., Loison, F., Mondal, S., Kocjan, P., Silberstein, L. E., Ding, S., and Luo, H. R. (2011). Pretreatment with phosphatase and tensin homolog deleted on chromosome 10 (PTEN) inhibitor SF1670 augments the efficacy of granulocyte transfusion in a clinically relevant mouse model. *Blood* **117,** 6702–6713.

Liot, G., Bossy, B., Lubitz, S., Kushnareva, Y., Sejbuk, N., and Bossy-Wetzel, E. (2009). Complex II inhibition by 3-NP causes mitochondrial fragmentation and neuronal cell death via an NMDA- and ROS-dependent pathway. *Cell Death Differ.* **16,** 899–909.

Liu, C. S., Tsai, C. S., Kuo, C. L., Chen, H. W., Lii, C. K., Ma, Y. S., and Wei, Y. H. (2003). Oxidative stress-related alteration of the copy number of mitochondrial DNA in human leukocytes. *Free Radic. Res.* **37,** 1307–1317.

Luengen, A. C., Friedman, C. S., Raimondi, P. T., and Flegal, A. R. (2004). Evaluation of mussel immune responses as indicators of contamination in San Francisco Bay. *Mar. Environ. Res.* **57,** 197–212.

Lunder, S., Hovander, L., Athanassiadis, I., and Bergman, A. (2010). Significantly higher polybrominated diphenyl ether levels in young U.S. children than in their mothers. *Environ. Sci. Technol.* **44,** 5256–5262.

Mariottini, M., Corsi, I., Della Torre, C., Caruso, T., Bianchini, A., Nesi, I., and Focardi, S. (2008). Biomonitoring of polybrominated diphenyl ether (PBDE) pollution: A field study. *Comp. Biochem. Physiol. C Toxicol. Pharmacol.* **148,** 80–86.

Martinez-Irujo, J. J., Villahermosa, M. L., Alberdi, E., and Santiago, E. (1996). A checkerboard method to evaluate interactions between drugs. *Biochem. Pharmacol.* **51,** 635–644.

Matsuno-Yagi, A., and Hatefi, Y. (1989). Uncoupling of oxidative phosphorylation: Different effects of lipophilic weak acids and electrogenic ionophores on the kinetics of ATP synthesis. *Biochemistry* **28,** 4367–4374.

McClain, V., Stapleton, H. M., Tilton, F., and Gallagher, E. P. (2012). BDE 49 and developmental toxicity in zebrafish. *Comp. Biochem. Physiol. C Toxicol. Pharmacol.* **155,** 253–258.

McDonald, T. A. (2002). A perspective on the potential health risks of PBDEs. *Chemosphere* **46,** 745–755.

Milgrom, Y. M., Ehler, L. L., and Boyer, P. D. (1991). The characteristics and effect on catalysis of nucleotide binding to noncatalytic sites of chloroplast F_1-ATPase. *J. Biol. Chem.* **266,** 11551–11558.

Miller, M. F., Chernyak, S. M., Batterman, S., and Loch-Caruso, R. (2009). Polybrominated diphenyl ethers in human gestational membranes from women in southeast Michigan. *Environ. Sci. Technol.* **43,** 3042–3046.

Mundy, W. R., Freudenrich, T. M., Crofton, K. M., and DeVito, M. J. (2004). Accumulation of PBDE-47 in primary cultures of rat neocortical cells. *Toxicol. Sci.* **82,** 164–169.

Murataliev, M. B., and Boyer, P. D. (1992). The mechanism of stimulation of MgATPase activity of chloroplast F_1-ATPase by non-catalytic adenine-nucleotide binding. Acceleration of the ATP-dependent release of inhibitory ADP from a catalytic site. *Eur. J. Biochem.* **209,** 681–687.

Naert, C., Van Peteghem, C., Kupper, J., Jenni, L., and Naegeli, H. (2007). Distribution of polychlorinated biphenyls and polybrominated diphenyl ethers in birds of prey from Switzerland. *Chemosphere* **68,** 977–987.

Napoli, E., Ross-Inta, C., Wong, S., Hung, C., Fujisawa, Y., Sakaguchi, D., Angelastro, J., Omanska-Klusek, A., Schoenfeld, R., and Giulivi, C. (2012). Mitochondrial dysfunction in Pten haplo-insufficient mice with social deficits and repetitive behavior: Interplay between Pten and p53. *PLoS ONE* **7,** e42504.

Offit, P. A. (2008). Vaccines and autism revisited–the Hannah Poling case. *N. Engl. J. Med.* **358,** 2089–2091.

Ohta, S., and Ohsawa, I. (2006). Dysfunction of mitochondria and oxidative stress in the pathogenesis of Alzheimer's disease: On defects in the cytochrome c oxidase complex and aldehyde detoxification. *J. Alzheimers Dis.* **9,** 155–166.

Okamoto, K., and Kondo-Okamoto, N. (2012). Mitochondria and autophagy: Critical interplay between the two homeostats. *Biochim. Biophys. Acta* **1820,** 595–600.

Oliveira, G., Diogo, L., Grazina, M., Garcia, P., Ataíde, A., Marques, C., Miguel, T., Borges, L., Vicente, A. M., and Oliveira, C. R. (2005). Mitochondrial dysfunction in autism spectrum disorders: A population-based study. *Dev. Med. Child Neurol.* **47,** 185–189.

Oros, D. R., Ross, J. R., Spies, R. B., and Mumley, T. (2007). Polycyclic aromatic hydrocarbon (PAH) contamination in San Francisco Bay: A 10-year retrospective of monitoring in an urbanized estuary. *Environ. Res.* **105,** 101–118.

Papadopoulou, L. C., Sue, C. M., Davidson, M. M., Tanji, K., Nishino, I., Sadlock, J. E., Krishna, S., Walker, W., Selby, J., Glerum, D. M., *et al.* (1999). Fatal infantile cardioencephalomyopathy with COX deficiency and mutations in SCO2, a COX assembly gene. *Nat. Genet.* **23,** 333–337.

Park, H. Y., Hertz-Picciotto, I., Sovcikova, E., Kocan, A., Drobna, B., and Trnovec, T. (2010). Neurodevelopmental toxicity of prenatal polychlorinated biphenyls (PCBs) by chemical structure and activity: A birth cohort study. *Environ. Health* **9,** 51.

Peça, J., Feliciano, C., Ting, J. T., Wang, W., Wells, M. F., Venkatraman, T. N., Lascola, C. D., Fu, Z., and Feng, G. (2011). Shank3 mutant mice display autistic-like behaviours and striatal dysfunction. *Nature* **472,** 437–442.

Pessah, I. N., Cherednichenko, G., and Lein, P. J. (2010). Minding the calcium store: Ryanodine receptor activation as a convergent mechanism of PCB toxicity. *Pharmacol. Ther.* **125,** 260–285.

Petreas, M., Nelson, D., Brown, F. R., Goldberg, D., Hurley, S., and Reynolds, P. (2011). High concentrations of polybrominated diphenylethers (PBDEs) in breast adipose tissue of California women. *Environ. Int.* **37,** 190–197.

Poot, M., Zhang, Y. Z., Krämer, J. A., Wells, K. S., Jones, L. J., Hanzel, D. K., Lugade, A. G., Singer, V. L., and Haugland, R. P. (1996). Analysis of mitochondrial morphology and function with novel fixable fluorescent stains. *J. Histochem. Cytochem.* **44,** 1363–1372.

Pun, R. Y., Rolle, I. J., Lasarge, C. L., Hosford, B. E., Rosen, J. M., Uhl, J. D., Schmeltzer, S. N., Faulkner, C., Bronson, S. L., Murphy, B. L., *et al.* (2012).

Excessive activation of mTOR in postnatally generated granule cells is sufficient to cause epilepsy. *Neuron* **75,** 1022–1034.

Reistad, T., Fonnum, F., and Mariussen, E. (2006). Neurotoxicity of the pentabrominated diphenyl ether mixture, DE-71, and hexabromocyclododecane (HBCD) in rat cerebellar granule cells in vitro. *Arch. Toxicol.* **80,** 785–796.

Roberts, S. C., Noyes, P. D., Gallagher, E. P., and Stapleton, H. M. (2011). Species-specific differences and structure-activity relationships in the debromination of PBDE congeners in three fish species. *Environ. Sci. Technol.* **45,** 1999–2005.

Roosens, L., Dirtu, A. C., Goemans, G., Belpaire, C., Gheorghe, A., Neels, H., Blust, R., and Covaci, A. (2008). Brominated flame retardants and polychlorinated biphenyls in fish from the river Scheldt, Belgium. *Environ. Int.* **34,** 976–983.

Ross-Inta, C., Omanska-Klusek, A., Wong, S., Barrow, C., Garcia-Arocena, D., Iwahashi, C., Berry-Kravis, E., Hagerman, R. J., Hagerman, P. J., and Giulivi, C. (2010). Evidence of mitochondrial dysfunction in fragile X-associated tremor/ataxia syndrome. *Biochem. J.* **429,** 545–552.

Schecter, A., Pavuk, M., Päpke, O., Ryan, J. J., Birnbaum, L., and Rosen, R. (2003). Polybrominated diphenyl ethers (PBDEs) in U.S. mothers' milk. *Environ. Health Perspect.* **111,** 1723–1729.

Schwarzenbach, R. P., Escher, B. I., Fenner, K., Hofstetter, T. B., Johnson, C. A., von Gunten, U., and Wehrli, B. (2006). The challenge of micropollutants in aquatic systems. *Science* **313,** 1072–1077.

Seo, J., Lee, N.-H., Shin, J.-H., Han, S.-Y., Jung, K.-K., Kang, I.-H., and Kang, Y. (2008). Dietary PBDE intake: A market-basket study in Korea. *Organohalogen Compd.* **70,** 2147–2150.

Shao, J., White, C. C., Dabrowski, M. J., Kavanagh, T. J., Eckert, M. L., and Gallagher, E. P. (2008). The role of mitochondrial and oxidative injury in BDE 47 toxicity to human fetal liver hematopoietic stem cells. *Toxicol. Sci.* **101,** 81–90.

She, J., Petreas, M., Winkler, J., Visita, P., McKinney, M., and Kopec, D. (2002). PBDEs in the San Francisco Bay Area: Measurements in harbor seal blubber and human breast adipose tissue. *Chemosphere* **46,** 697–707.

Shors, T. J., Miesegaes, G., Beylin, A., Zhao, M., Rydel, T., and Gould, E. (2001). Neurogenesis in the adult is involved in the formation of trace memories. *Nature* **410,** 372–376.

Sims, N. R., and Anderson, M. F. (2008). Isolation of mitochondria from rat brain using Percoll density gradient centrifugation. *Nat. Protoc.* **3,** 1228–1239.

Stapleton, H. M., Brazil, B., Holbrook, R. D., Mitchelmore, C. L., Benedict, R., Konstantinov, A., and Potter, D. (2006). In vivo and in vitro debromination of decabromodiphenyl ether (BDE 209) by juvenile rainbow trout and common carp. *Environ. Sci. Technol.* **40,** 4653–4658.

Ta, T. A., Koenig, C. M., Golub, M. S., Pessah, I. N., Qi, L., Aronov, P. A., and Berman, R. F. (2011). Bioaccumulation and behavioral effects of 2,2',4,4'-tetrabromodiphenyl ether (BDE-47) in perinatally exposed mice. *Neurotoxicol. Teratol.* **33,** 393–404.

Talsness, C. E., Shakibaei, M., Kuriyama, S. N., Grande, S. W., Sterner-Kock, A., Schnitker, P., de Souza, C., Grote, K., and Chahoud, I. (2005). Ultrastructural changes observed in rat ovaries following in utero and lactational exposure to low doses of a polybrominated flame retardant. *Toxicol. Lett.* **157,** 189–202.

Tchir, J., and Acker, J. P. (2010). Mitochondria and membrane cryoinjury in micropatterned cells: Effects of cell-cell interactions. *Cryobiology* **61,** 100–107.

Terada, H. (1981). The interaction of highly active uncouplers with mitochondria. *Biochim. Biophys. Acta* **639,** 225–242.

Thyagarajan, D., Shanske, S., Vazquez-Memije, M., De Vivo, D., and DiMauro, S. (1995). A novel mitochondrial ATPase 6 point mutation in familial bilateral striatal necrosis. *Ann. Neurol.* **38,** 468–472.

Trettel, F., Rigamonti, D., Hilditch-Maguire, P., Wheeler, V. C., Sharp, A. H., Persichetti, F., Cattaneo, E., and MacDonald, M. E. (2000). Dominant phenotypes produced by the HD mutation in STHdh(Q111) striatal cells. *Hum. Mol. Genet.* **9,** 2799–2809.

Tulinius, M., Moslemi, A. R., Darin, N., Westerberg, B., Wiklund, L. M., Holme, E., and Oldfors, A. (2003). Leigh syndrome with cytochrome-c oxidase deficiency and a single T insertion nt 5537 in the mitochondrial tRNATrp gene. *Neuropediatrics* **34,** 87–91.

van Boxtel, A. L., Kamstra, J. H., Cenijn, P. H., Pieterse, B., Wagner, J. M., Antink, M., Krab, K., van der Burg, B., Marsh, G., Brouwer, A., *et al.* (2008). Microarray analysis reveals a mechanism of phenolic polybrominated diphenylether toxicity in zebrafish. *Environ. Sci. Technol.* **42,** 1773–1779.

van Dam, K., and Slater, E. C. (1967). A suggested mechanism of uncoupling of respiratory-chain phosphorylation. *Proc. Natl. Acad. Sci. U.S.A.* **58,** 2015–2019.

van Praag, H., Schinder, A. F., Christie, B. R., Toni, N., Palmer, T. D., and Gage, F. H. (2002). Functional neurogenesis in the adult hippocampus. *Nature* **415,** 1030–1034.

Varga, E. A., Pastore, M., Prior, T., Herman, G. E., and McBride, K. L. (2009). The prevalence of PTEN mutations in a clinical pediatric cohort with autism spectrum disorders, developmental delay, and macrocephaly. *Genet. Med.* **11,** 111–117.

Vasilyeva, E. A., Fitin, A. F., Minkov, I. B., and Vinogradov, A. D. (1980). Kinetics of interaction of adenosine diphosphate and adenosine triphosphate with adenosine triphosphatase of bovine heart submitochondrial particles. *Biochem. J.* **188,** 807–815.

Verny, C., Guegen, N., Desquiret, V., Chevrollier, A., Prundean, A., Dubas, F., Cassereau, J., Ferre, M., Amati-Bonneau, P., Bonneau, D., *et al.* (2011). Hereditary spastic paraplegia-like disorder due to a mitochondrial ATP6 gene point mutation. *Mitochondrion* **11,** 70–75.

Wang, F., Liu, W., Jin, Y., Dai, J., Zhao, H., Xie, Q., Liu, X., Yu, W., and Ma, J. (2011). Interaction of PFOS and BDE-47 co-exposure on thyroid hormone levels and TH-related gene and protein expression in developing rat brains. *Toxicol. Sci.* **121,** 279–291.

Weinbach, E. C., and Garbus, J. (1969). Mechanism of action of reagents that uncouple oxidative phosphorylation. *Nature* **221,** 1016–1018.

Wilson, D. F., and Merz, R. (1969). Inhibition of mitochondrial respiration by uncouplers of oxidative phosphorylation. II. The site of inhibition of succinate oxidation by the uncouplers. *Arch. Biochem. Biophys.* **129,** 79–85.

Yonetani, T., and Theorell, H. (1964). Studies on liver alcohol hydrogenase complexes. 3. Multiple inhibition kinetics in the presence of two competitive inhibitors. *Arch. Biochem. Biophys.* **106,** 243–251.

Zhang, S., Bursian, S., Martin, P. A., Chan, H. M., and Martin, J. W. (2008). Dietary accumulation, disposition, and metabolism of technical pentabrominated diphenyl ether (de-71) in pregnant mink (Mustela vison) and their offspring. *Environ. Toxicol. Chem.* **27,** 1184–1193.

Zhou, J., Blundell, J., Ogawa, S., Kwon, C. H., Zhang, W., Sinton, C., Powell, C. M., and Parada, L. F. (2009). Pharmacological inhibition of mTORC1 suppresses anatomical, cellular, and behavioral abnormalities in neural-specific Pten knock-out mice. *J. Neurosci.* **29,** 1773–1783.

Zhou, T., Taylor, M. M., DeVito, M. J., and Crofton, K. M. (2002). Developmental exposure to brominated diphenyl ethers results in thyroid hormone disruption. *Toxicol. Sci.* **66,** 105–116.

Zota, A. R., Rudel, R. A., Morello-Frosch, R. A., and Brody, J. G. (2008). Elevated house dust and serum concentrations of PBDEs in California: Unintended consequences of furniture flammability standards? *Environ. Sci. Technol.* **42,** 8158–8164.